Physica Scripta. Vol. XX, 1–4, 2003

f705 Date: 4/2/03 Time 10:41am 1st Proof

Multiple Beam Interference of Light in an Absorbing Wedge

V. C. Vani[1,*]

[1] Department of Instrumentation, Indian Institute of Science, Bangalore 560 012, India

Received June 18, 2002; accepted December 5, 2002

PACS Ref: 42.15Dp, 42.25Fx, 42.25Hz

Abstract

Multiple beam interference of light in a wedge is considered when the wedge is filled with an absorbing medium.The aim is to examine a method that may give values of both the real and the imaginary parts of the refractive index of the absorbing medium. We propose here a method to determine these quantities from simple techniques like fringe counting and interferometry, by using as the incident wave either a single Gaussian beam or two parallel Gaussian beams. This method gives good results even when the absorption coefficient is high. The analysis of the method begins with an analysis of the intensity distribution for rays emerging from a wedge shaped thin film, when several beams are incident on the wedge and are allowed to have multiple reflections in the wedge.

We hope to use this method in surface profiling.

1. Introduction

Intensity patterns as produced by multiple reflections in a transparent plane wedge is a subject of interest in various contexts of optics [1,2]. The need for considering a wedge is in fact two fold. Firstly in making large surfaces, errors of the order of 10^{-3} radians are difficult to avoid and secondly by using a wedge one can increase the dispersive properties of the system which improves the accuracy with which the real and imaginary parts of the refractive index can be measured. In our present analysis the refractive and absorptive properties of the dielectric medium are expressed by a complex refractive index. The calculation of the intensity pattern requires the proper evaluation of the path lengths of the different rays that emerge from the wedge such that one can find the electric field, by taking into account the proper amplitude and phase for every emergent ray [3–5]. The situation generally encountered is shown in Fig. 1. The intensity pattern is very sensitive to the phases of the different rays and therefore a proper calculation of the path lengths is necessary. Calculation of this path length also helps to find the amplitude of the wave as it emerges from the wedge, by simply putting an attenuation factor in the different rays, consistent with the path lengths that they have travelled.

The aim here is to show that determination of both the real and imaginary parts of the refractive index is possible from simple techniques like fringe counting and intensity pattern matching for multiple beam interferometry. As a test case we consider the optical properties of a material close to its absorbing frequency, i.e., where the imaginary part of the refactive index dominates. It is seen that multiple reflections of a single beam produce a flattened intensity distribution from which it is diffcult to extract the real part of the refractive index. However, an interferometry experiment with two incident beams is suggested to determine the real and imaginary parts of the refractive index. Both the beams are allowed to have multiple reflections in the slab and the interference is allowed to take place between all the emergent beams from the slab.

2. Theory

The theoretical expressions for the intensity are obtained from the calculational methods given recently by the present author [6], with the addition that for every emergent ray the amplitude has to be calculated by incorporating an appropriate attenuation factor, consistent with the absorption coefficient as also the path length of the respective rays. We reproduce the main intensity expression here for completeness and clarity in the subsequent discussions.

We refer to Fig. 1 and consider a ray incident at A. For the first emergent ray, the phase is given by

$$\psi(0) = 2\pi\rho/\lambda[\mu_1 \sin\theta_1 + \mu_2 \sin\alpha/\cos(\alpha+\theta')] \tag{1}$$

and it emerges from the point

$$x(0,\rho) = \rho\cos\theta'/\cos(\alpha+\theta') \tag{2}$$

The angle θ' satisfies Snell's law

$$\mu_1 \sin\theta = \mu_2 \sin\theta'. \tag{3}$$

The second beam travels an extra path CDE $\equiv \delta 1(\rho)$

$$= 4\rho\sin\alpha\cos\alpha\cos\theta'/[\cos 2\alpha + \cos(2\theta'+4\alpha)] \tag{4}$$

and emerges from

$$x(1,\rho) = \rho\cos\theta'/\cos(3\alpha+\theta') \tag{5}$$

Similar calculations based on simple geometry of triangles show that the pth ray emerges from

$$x(p,\rho) = \rho\cos\theta'/\cos[(2p+1)\alpha+\theta'] \tag{6}$$

after travelling a total path $L(p,\rho)$ in the wedge such that

$$\delta l(p,\rho) = L(p+1,\rho) - L(p,\rho)$$
$$= 4\rho\sin\alpha\cos\alpha\cos\theta'/[\cos 2\alpha + \cos(2\theta'+4p\alpha)] \tag{7}$$

* e-mail: vani@isu.iisc.ernet.in, chat@bgl.vsnl.net.in

© Physica Scripta 2003

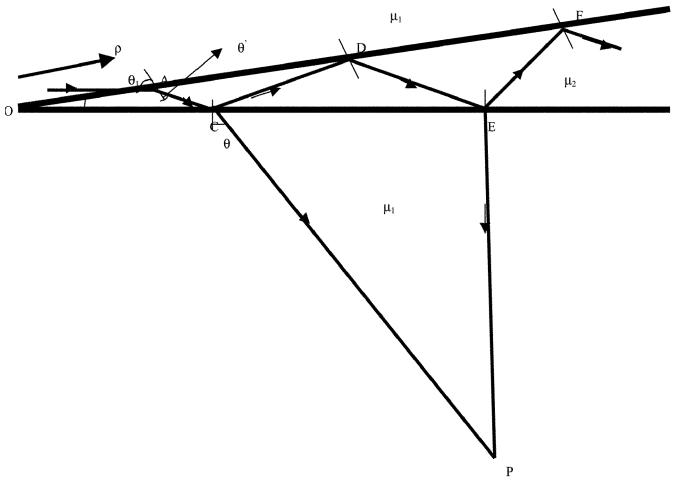

Fig. 1. Sketch of the optics of the system. All calculations and computations are based on this geometry.

It is thus clear that for the pth emergent ray the total path length in the wedge is found over the entire zig-zag path and is thus found from its sum.

$$L(p,\rho) = \sum_{k=1}^{p} \delta 1(k) = \delta l(\rho) + \int_{k=1}^{p} \delta 1(k,\rho)\,\mathrm{d}k \tag{8}$$

where we are using an Euler–Maclaurin summation formula, giving

$$\begin{aligned} L(p,\rho) = {} & \delta l(\rho) + \pi(\rho\cos\theta'/\alpha) \\ & \times \ln[(1+\cos 2\alpha + \sin 2\alpha\tan(2p\alpha+\theta')) \\ & \times (1+\cos 2\alpha - \sin 2\alpha\tan(2\alpha+\theta'))/ \\ & \times (1+\cos 2\alpha + \sin 2\alpha\tan(2\alpha+\theta')) \\ & \times (1+\cos 2\alpha - \sin 2\alpha\tan(2\alpha+\theta'))] \end{aligned} \tag{9}$$

This sum given in (9) is a good approximation, whenever the terms in the sum do not oscillate rapidly with p, i.e., when $\cos\alpha \ll 1$ and $\cos\alpha p \ll 1$. Thus, every emergent beam arrives at p, with a phase,

$$\begin{aligned} \psi(p,\rho) &= \psi(\rho,0) + (2\pi/\lambda)L(p,\rho)\mu_{2\mathrm{r}} - (2\pi/\lambda)x(p,\rho)\sin\theta\mu_1 \\ &= (2\pi/\lambda)\rho\chi(p,\theta) \end{aligned} \tag{10}$$

in the limit of Fraunhofer diffraction.

Here $\mu_{2\mathrm{r}}$ is the real part of the refractive index of medium 2. This part gives rise to only the phase shift. The imaginary part of the refractive index of the wedge gives rise to attenuation, so that the amplitude of the pth emergent ray is $r^p \mathrm{e}^{-\mu}_{2\mathrm{i}L(p,\rho)}$. We further consider two rays incident at $\rho = \rho_{\mathrm{c}1}$ and $\rho_{\mathrm{c}2}$ respectively. The waves from each of these two rays get divided on multiple reflection.

We consider the incident beam to be a Gaussian, coherent one, with an electric field distribution with ρ being

$$P(\rho) = \left(1/\sqrt{\pi}\Delta\right)\exp\left(-(\rho-\rho_{\mathrm{c}})^2/\Delta^2\right) \tag{11}$$

The net electric field contribution is, on adding over all ρ's calculated as follows.

We designate as E_1 and E_2 the first emergent rays: They add up to give a field,

$$\begin{aligned} E_1 + E_2 = {} & \int_{-\infty}^{+\infty} \exp(\mathrm{i}(\rho_1 - \rho_{\mathrm{c}1} + \rho_{\mathrm{c}1})(a+\mathrm{i}b)) \\ & \times \exp(-(\rho_1-\rho_{\mathrm{c}1})^2/\Delta^2 \mathrm{d}\rho_1) \\ & + \int_{-\infty}^{+\infty} \exp(\mathrm{i}(\rho_1 - \rho_{\mathrm{c}1} + \rho_{\mathrm{c}1})(a+\mathrm{i}b)) \\ & \times \exp(-(\rho_1-\rho_{\mathrm{c}1})^2/\Delta_2^2\,\mathrm{d}\rho_2). \end{aligned} \tag{12}$$

In a similar way, the waves from the rest of the emergent rays, owing to multiple reflections contribute,

$$\begin{aligned} E_3 + E_4 = {} & \sum_{p=1}^{\infty}[\exp(-\beta p)\int_{-\infty}^{+\infty} \\ & \times \exp(\mathrm{i}(\rho_1 - \rho_{\mathrm{c}1} + \rho_{\mathrm{c}1})(c+\mathrm{i}d)) \\ & \times \exp(-(\rho_1-\rho_{\mathrm{c}1})^2/\Delta_1^2 \mathrm{d}\rho_1) \\ & + \exp(-\beta p)\int_{-\infty}^{+\infty} \exp(\mathrm{i}(\rho_1 - \rho_{\mathrm{c}1} + \rho_{\mathrm{c}1})(c+\mathrm{i}d)) \\ & \times \exp(-(\rho_1-\rho_{\mathrm{c}1})^2/\Delta_2^2\,\mathrm{d}\rho_2)]. \end{aligned} \tag{13}$$

Above,

$$\begin{aligned} a &= [\mu_1\sin\theta_1 + \mu_2\sin\alpha/\cos(\alpha+\theta') \\ &\quad - \mu_3\cos\theta'\sin\theta/\cos(\alpha+\theta')]2\pi/\lambda, \\ b &= \mu_{2\mathrm{i}}\sin\alpha/\cos(\alpha+\theta'), \\ c &= (2\pi/\lambda)[\mu_1\sin\theta_1 + \mu_{2\mathrm{r}}\sin\alpha/\cos(\alpha+\theta')] \\ &\quad + \mu_2 f(p) - \mu_3 f_1(p), \\ d &= \mu_{2\mathrm{i}} f(p). \end{aligned} \tag{14}$$

The total field is thus $E_{\mathrm{tot}} = E_1 + E_2 + E_3 + E_4$, which on integration gives the complex field

$$\begin{aligned} E_{\mathrm{tot}} = \sqrt{\pi}\Big[& \exp(\mathrm{i}(a-b)\rho_{\mathrm{c}1})\exp\left((a+\mathrm{i}b)^2\Delta_1^2/4\right)\Delta_1 \\ & + \exp(\mathrm{i}(a-b)\rho_{\mathrm{c}2})\exp\left((a+\mathrm{i}b)^2\Delta_2^2/4\right)\Delta_2 \\ & + \sum_{p=1}^{\infty}\exp(-\beta p)\exp((\mathrm{i}c-d)\rho_{\mathrm{c}1}) \\ & \times \exp\left((c+\mathrm{i}d)^2\Delta_1^2/4\right)\Delta_1 \\ & + \sum_{p=1}^{\infty}\exp(-\beta p)\exp((\mathrm{i}c-d)\rho_{\mathrm{c}2}) \\ & \times \exp\left((c+\mathrm{i}d)^2\Delta_2^2/4\right)\Delta_2\Big] \end{aligned} \tag{15}$$

© Physica Scripta 2003

as expected considering the Gaussian nature of the integrals. The intensity at any point is given by

$$I(\rho, \alpha, \theta_1; \theta) = |E_{\text{tot}}(\rho, \alpha, \theta_1; \theta)|^2. \tag{16}$$

The Gaussian factor $\exp\left(-(2\pi\Delta\chi(p,\theta)/2\lambda)^2\right)$ tends to center every term in the sum around the values of θ, such that $(2\pi\Delta\chi(p,\theta)/2\lambda)^2 \ll 1$, as expected due to diffraction for any finite Δ. Thus by making Δ sufficiently small, these term may have considerable sweep over θ, as in the present case, where we have chosen $\Delta \approx 1\,\mu$ for $\lambda = 6328$ Å. It is to be understood that the Gaussian factor in (15) arises because we have considered a Gaussian beam. For other kinds of beams, however, this Gaussian factor has to be replaced by an appropriate factor consistent with the amplitude and phase distribution in the incident beam. It can be seen that the $p = 0$ term is centered around $\Psi(0) - (2\pi/\lambda)x_0 \sin\theta = 0$, which is exactly the geometrical optics formula for the emergent ray θ, as given by the well known formula for a prism. However, due to the finite size of the Gaussian beam, there is a spread of intensity around this central ray, the central ray direction being given by the prism formula. For different p values, the Gaussian factors are centered around $\chi(p,\theta) = 0$, i.e., give maxima in different θ directions, implying that the different emergent rays from the wedge are not parallel to each other if α be non zero.

The factors $\exp(\mathrm{i}\Psi(p, \rho_c))$ in the different terms in the sum are the "phase terms" which give rise to interference terms in (14). The interference results for thin films $d \leq 50\,\mu$m and low wedge angles, $\alpha \leq 0.01$ radians, are now studied, with the aid of Eq. (14). It is to be noted that the formula becomes inaccurate for $\alpha > 0.03$ radians as the summation given by the Euler–Mclaurin expression (8,9) then requires a larger number of terms to be added, a step that will be taken up in a future communication.

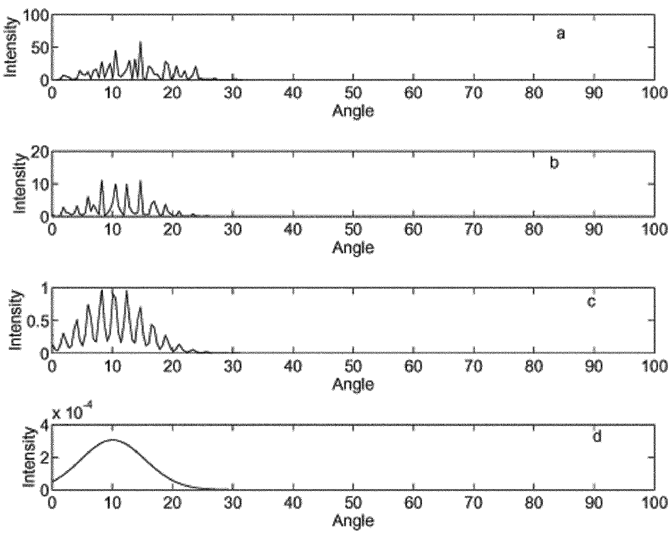

Fig. 2. Effect of absorption on the intensity of light. This figure shows a plot of the scattering angle vs. intensity. The four plots give intensity profiles for different refractive indices.

Refractive index $= 1.0 + (1 \cdot 10^{-5}\,\mathrm{i})$.
Refractive index $= 1.0 + (1 \cdot 10^{-4}\,\mathrm{i})$.
Refractive index $= 1.0 + (1 \cdot 10^{-3}\,\mathrm{i})$.
Refractive index $= 1.0 + (1 \cdot 10^{-2}\,\mathrm{i})$.

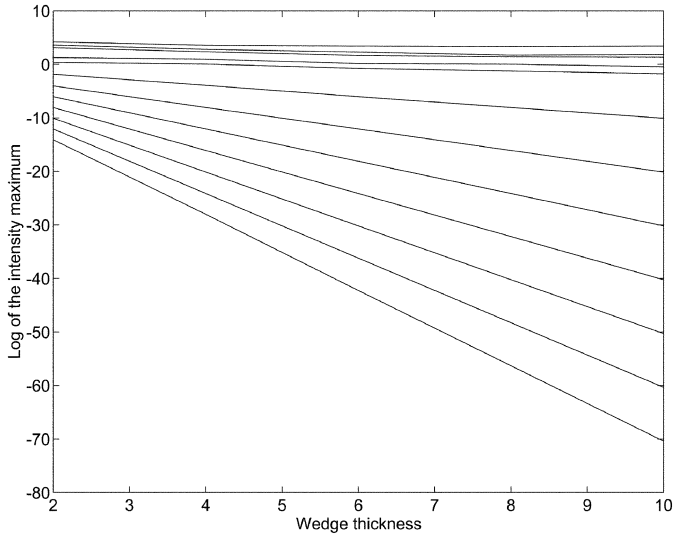

Fig. 3. Plot of the wedge thickness vs. the logarithm of the maximum value of the intensity at a given value of the imaginary part of the refractive index. The imaginary part of the refractive index varies from $1 \cdot 10^{-5}$ to 10^{-2} and the real part is kept constant at 1.1.

3. Results and discussion

The issues involved here are a combination of both diffraction and interference of light. The width Δ of the beam defines the width of the diffraction profile, being given by $\Delta\theta \approx \lambda/\Delta$ while the separation between the fringes due to interference is nearly $\delta\theta \approx \lambda/d$. Thus the number of interference fringes that can be accommodated in the diffraction envelope is $n \approx \Delta\theta/\delta\theta = d/\Delta$ (apart from factors that depend on the angle of incidence), so it is essential that in order that the fringe count method be effective $n \geq 4$. This puts the limitations on the application of the method due to limitations of obtaining apertures with sufficiently small Δ. In absence of the wedge, the interference should be exactly as that of a Fabry–Perot, if the wedge angle is absent and if the light is allowed to arrive at all possible angles, i.e. if α and Δ are both very small.

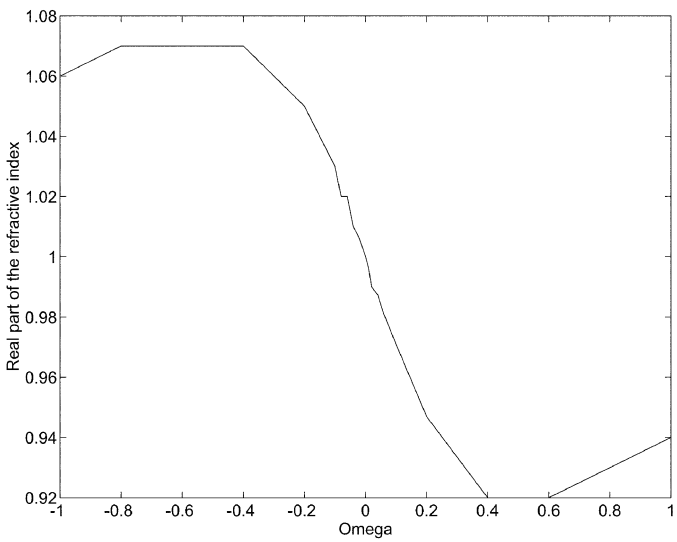

Fig 4. Plot of omega vs. the real part of the refractive index. The relation between omega and the refractive index is given in the text.

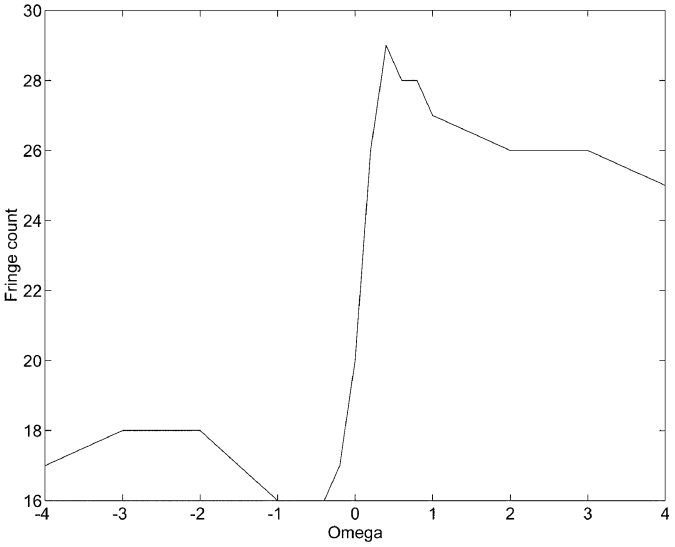

Fig. 5. Plot of omega vs. the fringe count after a reference point. The relation between omega and refractive index is given in the text.

The effect of absorption on the intensity of the light is shown in Figs. 2 and 3. In Fig. 2 we see that for a fixed wedge angle and angle of incidence, the intensity decreases as the absorption increases, as is expected. We also see that as we go from Figs. 2(a) to (d) (which is in the order of increasing absorption) the number of fringes also decreases, forcing us to use two incident beams for getting useful information at high absorption. Figure 3 also shows the decrease of the intensity maximum as the absorption increases.

The determination of the real and imaginary parts of the refractive index completely characterises the given system. The real part decides the phase of the light beam as it travels in the medium and the imaginary part determines the attenuation of the amplitude of the wave.

The role of the imaginary part of the refractive index is shown in Fig. 3. The real part of the refractive index is kept constant and the imaginary part is varied over a wide range for different thicknesses of the wedge. The plot of the wedge thickness verses the log of the intensity maximum is a straight line for all values of the refractive index (imaginary). These straight lines for a given wedge can be calibrated to give an accurate value of the imaginary part of the refractive index.

Determination of the real part of the refractive index involves fringe counting with the incidence of two beams at slightly different distances from the apex of the wedge. This is because when a single beam is used at high absorption values, only a broad peak is obtained and we can not extract any information.

The computations in Figs. 4 and 5 were carried out using the following relations. As mentioned earlier the computations are carried out in a small range where the absorption is optimised.

$$\mu_r = n_0 + (4\pi e^2/n_0 m\omega'_s)((Nf_s)(\omega_s - \omega)/(4(\omega'_s - \omega)^2 + \gamma_s^2)),$$

$$\mu_i = 1//\mu_r[(2\pi e^2/n_0 m\omega'_s)((Nf_s)\gamma_s/4(\omega'_s - \omega)^2 + \gamma_s^2)]$$

Author Queries

Ref. 1 - Spelling of Castaneda/Castenada

? Check Fig. 1 please.

where

μ_r = real part of the refractive index,

μ_i = imaginary part of the refractive index,

ω_s = absorption frequency = $7.4 \cdot 10^{15}\,s^{-1}$,

$\gamma_s = 3.3 \cdot 10^{11}\,s^{-1}$,

$Nf_s = 9.2 \cdot 10^{16}\,cm^{-3}$,

e = electronic charge = $4.80325 \cdot 10^{-10}$ esu,

m = electronic mass = $9.10956 \cdot 10^{-28}$ gms.

Figures 4 and 5 show a plot of ω vs. the real part of the refractive index and ω vs the fringe count after a reference point. In this case we have used as fringe count the number of intensity maxima that appear after the reference point. We note from Figs. 4 and 5 that the fringe count vs. ω has a shape similar to the curve which gives the variation of the real part of the refractive index with the frequency ω of the incident light. This shows that fringe count helps us to obtain an idea about the behaviour of the real refractive index and can get an approximate estimate of the real refractive index. An accurate estimation of the real refractive index would involve fitting the intensity values to Eq. (16).

The work described here also has direct relevance to scattering by absorbing flakes and follows the analysis presented in Ref. [7]. It is to be noted that our analysis can be applied to flakes of fairly large size so that the cross sectional area of the flake is greater than the cross sectional area of the incident beam. This approximation allows one to neglect the scattering at the edges [8,9]. We plan to extend the above analysis to incorporate the effct of the edges and the effect of roughness on the intensity pattern of the transmitted light. As a first approximation, the latter can be admitted by choosing a suitable distribution and considering its autocorrelation. Such an averaging will smear out the intensity distribution, given in Eqs. (15) and (16). However, observations conducted at multiple wavelengths, as suggested in Ref. [10], are likely to reveal the parameters of the system.

References

1. Castaneda, R. and Castenada, J. G. S. R., Appl. Opt. **38**, 6522 (1999).
2. Chandra, V. S. and Pechereky, M. J., Opt. Engg. **38**, 1743 (1999).
3. Malacara, D., "Optical Shop Testing," (John Wiley and Sons, 1992).
4. Born, M. and Wolf, E., "Principles of Optics," (Cambridge University Press, Chapter 7, 1999).
5. Francon, M., "Optical Interferometry," (Academic Press, 1966).
6. Vani, V. C., Ind. J. Phys. **75B**, 433 (2001).
7. Waldemarsson, K. W. T. and Gustafson, B. A. S., "Fifth International Conference on Light Scattering by Non Spherical Particles," (Edited by Videen, S., Fu, Q. and Chylek, P.), (Army Research Lab. Press, Adelphi, Maryland, 2000) p. 34.
8. Kuryoumjian, R. G. and Pathak, P. H., Proc. IEEE. **62**, 1448 (1974).
9. Syed, H. H. and Volakis, J. L., Radio Science **30**, 505 (1995).
10. Chatterjee, S., Ind. J. Phys. **74B**, 363 (2000).

 © *Physica Scripta 2003*